

Application of a semiquantitative and GIS-based statistical model to landslide susceptibility zonation in Kayangan Catchment, Java, Indonesia

Danang Sri Hadmoko¹ · Franck Lavigne² · Guruh Samodra¹

Received: 31 March 2015 / Accepted: 30 January 2017 / Published online: 13 February 2017
© Springer Science+Business Media Dordrecht 2017

Abstract Kayangan Catchment, one of the extremely landslide susceptible areas in Indonesia, is situated on the eastern flank of Menoreh Mountain in Yogyakarta Province on the island of Java. Landslides cause land and infrastructure damages because of their frequency in human settlements. The objectives of this study are twofold: (1) to analyze the spatial distribution of landslides and its correlation using terrain parameters; and (2) to analyze landslide susceptibility using both semiquantitative and statistical methods, i.e., analytical hierarchy process (AHP) and information value (IV) methods. Nine parameter maps were introduced to assess landslide susceptibility. The parameter maps and landslide distribution map were spatially overlaid to calculate the contribution of each parameter to landslide susceptibility. The landslide susceptibility map encompassed four different categories: very high, high, medium, and low susceptibility. The map was validated through a success rate curve by determining the area under the curve using existing landslide events. The success rate curves indicated that the IV was more accurate than the AHP, although both of them had high correlations. Both methods show that the precondition factors represented approximately 80% of the influence on landslide occurrence, with the remaining 20% attributed to the triggering factors, primarily rainfall and seismic factors.

Keywords Landslide susceptibility · Statistical method · Analytical hierarchy process · Information value · GIS

✉ Danang Sri Hadmoko
hadmoko@ugm.ac.id

¹ Department of Geography and Environmental Science, Faculty of Geography, Universitas Gadjah Mada, Sekip-Bulaksumur, Yogyakarta 55281, Indonesia

² UMR 8591 CNRS Laboratoire de Géographie Physique, University Paris 1 Panthéon Sorbonne, 1 Place A. Briand, 92195 Meudon Cedex, France

1 Introduction

Landslides are major natural hazards that often result in human and economic losses as a consequence of natural forces and human actions. Due to their high magnitude, rates of recurrence, and their high variability of reporting and documenting in different nations, the economic losses and casualties caused by landslides are greater than commonly known (Sidle and Ochiai 2006; García-Rodríguez et al. 2008). In addition, the loss of property is greater than that from any other natural disaster, including earthquakes, floods, and windstorms (García-Rodríguez et al. 2008). In Java, for example, more than 1400 landslides have been inventoried during the period 1981–2007. They have caused estimated 2095 casualties and 552 human injuries (Hadmoko 2009; Hadmoko et al. 2010).

At present, loss of life and properties because of landslides in Java as well as in many areas in the world appears to be increasing, mainly because of an increase in population and urbanization in hazardous locations; thus, a landslide hazard mitigation program is necessary. The reduction in the impacts of landslides is therefore a topic of major interest for both geoscientists and engineering professionals as well as for the community and the local administrations in many parts of the world (Aleotti and Chowdhury 1999). To perform proper landslide mitigation, comprehensive information regarding landslides, such as occurrence, spatial distribution, and susceptibility, is needed. This information is essential for determining landslide zones before any human activities or infrastructures are installed, so that adequate control measures can be properly implemented.

Landslides are the result of two sets of factors: precondition factors, which are generally naturally induced and relatively constant over time and which govern the stability conditions of slopes; and preparatory and triggering factors, which are relatively dynamic, induced either by natural factors or by human intervention (Glade and Crozier 2005). Precondition factors are generally related to slope, lithology, geological structure, soil, and vegetation, whereas the preparatory and triggering factors are associated with a variety of external stimuli, such as intense rainfall, earthquake shaking, water-level change, storm waves, or rapid erosion, which decrease in the stability of the slope material (Dai et al. 2002).

To understand where future landslides will occur, an area may be divided into sub-areas that have homogenous properties, which are classified and ranked according to the degrees of potential hazard due to mass movements by considering the previously explained precondition factors (Varnes 1984). A map of this type is generally called landslide susceptibility zonation (LSZ) (Saha, et al. 2005). In the last 20 years, various methods have been developed and applied to the assessment of landslide hazards and risks, from the simplest method using the limited number of parameter and qualitative assessment to very sophisticated methods, using a large number of landslide parameter and quantitative formulas (van Westen 1993; Terlien 1996; Saha et al. 2005). One of the simplest approaches for analyzing landslide susceptibility is the qualitative method. In this method, subjective assessment rules are used to delineate the susceptible areas. The weighting and rating of landslide-influencing factors were decided based on expert knowledge (Saha et al. 2002). This method is widely used for the very remote areas for which landslide inventory maps remain unavailable. To remove the subjectivity of expert opinion in the determination of landslide susceptibility, a statistical approach is used. The approach considers both a landslide inventory map and landslide-influencing-factor maps.

The tremendous development of landslide hazard research is supported by the availability of remote sensing and geographic information system (GIS) technologies. GIS and

remote sensing have proven to be a versatile tool to manage spatial data and have become the current state of the art in landslide hazard and risk assessment (Van Westen et al. 2008). Through the appropriate use of GISs, most approaches to landslide susceptibility mapping enable the total automation of assessment and the standardization of data management techniques and allow us to build more efficient and accurate maps (He and Beighley 2008). This is because it is possible to acquire, store, query, manipulate, analyze, and display a set of spatial and non-spatial data regarding the influencing factors of landslides through these technologies (Carrara et al. 1991; Saha et al. 2002, 2005).

Some landslide studies were conducted in Indonesia with different perspectives and approaches, ranging from mapping spatiotemporal landslide occurrence in Java Island (e.g., Marfai et al. 2008; Hadmoko 2009) to assessing landslide triggering mechanism (e.g., Ahmed et al. 2013; Faris and Fawu 2014). These researches deal with the role of seismic and rainfall on landslide triggering process. However, very limited studies have been conducted on quantitative assessment of landslide susceptibility in Indonesia except some papers dealt with some natural factors (e.g., slope gradient, slope aspect, curvature map, and distance from stream) without incorporating any human intervention (e.g., Oh et al. 2010). This present contribution attempts to provide more comprehensive factors by coupling the natural factors as well as human interventions as the main predisposition factor for landslide susceptibility. Particularly in the study area, several researches have been conducted by some scientists (e.g., Hadmoko 2009; Hadmoko et al. 2009, 2010). A study on landslide distribution analysis and its relation with some parameter maps (e.g., DEM and its derivative maps, geology, land use at Kayangan Catchment were done at 1:25,000 scale (Hadmoko et al. 2009). Another study was also conducted at 1:50,000 scale for the entire area of Menoreh Mountains on landslide risk assessment and its implication on mitigation measure (Hadmoko et al. 2010). A semiquantitative method was applied in this research through scoring and weighting approach. A validation process was done by calculating the landslide density for entire research area. In spite of some studies conducted in the research area, a research focus on quantitative approach is still missing. This approach is very rarely applied in Indonesia because the data on landslide inventory map are still limited. This present contribution therefore provides a new insight on how to assess the landslide susceptibility by quantitative approaches with complete landslide dataset.

The aims of the study were to determine the spatial distribution of landslides and to compare them with the preconditioning factors to build landslide susceptibility maps by combining both natural and human factors. Special attentions were given on the application and comparison between semiquantitative method and bivariate statistical methods, i.e., the analytical hierarchy process (AHP) method and the information value model. These both methods have been widely applied by many scientists; however, no researcher has given attention to comparative study of both methods. This study also highlighted accuracy and reliability assessment in the classification of areas prone to landslides.

2 Study area

Situated approximately 30 km west of Yogyakarta City, Kayangan Catchment is positioned on the eastern flank of the Menoreh Mountains, Yogyakarta Province, on the island of Java (Fig. 1). With an area of 35.5 km², the study area is characterized by complex terrain and dominated by hilly and mountainous areas; it extends from an elevation of 49 m a.s.l. in the southern part, in the plain area of Tegalsari village, to 825 m a.s.l. in the

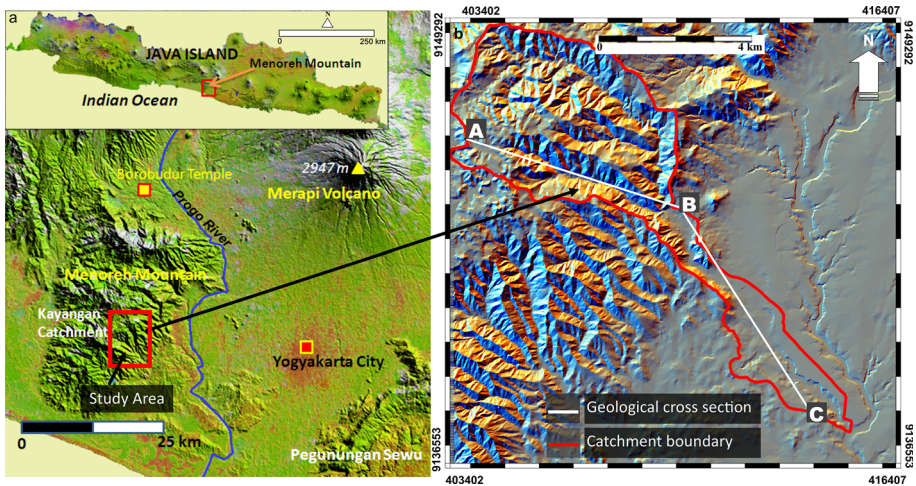


Fig. 1 Landscape of Kayangan Catchment of Central Java; the study area is marked by red rectangle (left-hand side, a) and red polylines showing the boundary of the catchment (b)

northern part, in the Ngori mountainous area (Hadmoko et al. 2009). The upper part of the catchment is characterized by steep, near-vertical slopes (>70°) within very deep valleys due to very intense denudational processes.

The climate of Kayangan is characterized by a humid tropical environment, as in other areas of Java. There are two pronounced seasons: a rainy season from November to April and a dry season from May to October. The annual rainfall ranges between 1500 and 3000 mm, and the average annual temperature is 29 °C. There is no significant difference between the temperature in the wet season and in the dry season, as in other areas in the tropics. This humid tropical climate accelerates the weathering of materials and landslide events.

Kayangan catchment consists of 6 geological formations: (1) the Kebobutak Formation (Tmok) consists of tertiary andesitic breccias, tuff, lapilli tuff, agglomerates, and andesitic lava flows; (2) the Jonggrangan Formation (Tmj) is dominated by conglomerated, tuffaceous marl and calcareous sandstone, limestone, and coralline limestone; (3) the Nanggulan Formation (Teon) is characterized by the presence of sandstone with intercalation of lignite, sandy marl, claystone with limonite concretion, intercalations of marl and limestone, sandstone, and tuff; (4) the Sentolo Formation (Tmps) consists of limestone and marly sandstone; (5) Qolluvium (Qc) consists of unsorted debris from Kebobutak Formation, and (6) the Old Andesite Formation (a) consists of weathered lava andesite

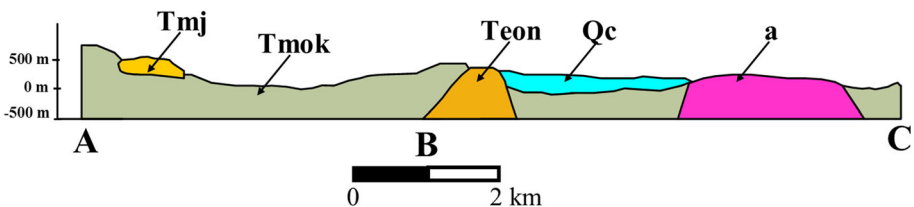


Fig. 2 Geological cross section of the study area consisting of (a) Jonggrangan Formation (Tmj), Kebobutak Formation (Tmok), Nanggulan Formation (Teon), Colluvium (Qc) and Old Andesite Formation (A)

covering the major part of study area (Rahardjo et al. 1995) (Figs. 2, 5e). Colluvial and alluvial deposits are primarily distributed across the middle and lower Kayangan Catchment as the result of depositional processes from eroded soils and regolith. The area is tectonically active as suggested by a number of active major and minor faults (Rahardjo et al. 1995). The density of deeply incised streams, temperature, and the high intensity of the rainfall are the major factors that contribute to the intense weathering and erosion processes in the study area.

On top of those geomorphic and geological setting, the study area is also characterized by human intervention that are represented by the presence of road networks, settlements, and agricultural area. Slope modification is very common in this area that triggers erosional process as well as landslides. Rice field is also very important land-use type of the study area that was host of some destructive landslide processes.

The study area was chosen for several reasons. The first reason is the frequent recurrence of landslides. A total of 131 shallow landslides during the time span of 2007–2009, which caused damage to houses and roads, were mapped for the entire area of Kayangan (Hadmoko 2009). Several types of landslides were inventoried (e.g., rockfall, sliding, slump, and soil creep) by their physical appearance, such as the morphology of the sliding surface, the landslide materials, the impacts on infrastructure, and the presence of a nearly vertical slope. Landslide in the study area becomes annual events that occur mainly during the peak of rainy season (December–February). Second, this study would provide spatial information of landslide as the primary input for a disaster risk reduction program. Third, the settlement area is expanding due to population growth; thus, correct information regarding safe areas is absolutely required.

3 Materials and methods

This study was performed in four major steps: (a) landslide data inventory, (b) spatial database management, (c) landslide susceptibility assessment, and (d) map validation (Fig. 3). The data, data sources, and methods are summarized in Table 1.

3.1 Landslide data inventory

Landslide data inventory was the first step performed in this study (Fig. 3a). Intensive fieldworks were undertaken from 2007 to 2009 to map and measure the spatial distribution of shallow landslides occurring during 2007, 2008, and 2009. These landslides were characterized by having a sliding surface that was located within the root zone or soil mantle. The landslides occurred during 2007 and 2008 were used for the susceptibility assessment (131 events), and the landslide occurred during 2009 was introduced for validation (46 events).

3.2 Spatial database management

Spatial information of landslide and factors that cause landslides, such as the slope, elevation, aspect, lithology, fault line, drainage network, road network, and land use was used as the main factors controlling landslides (Chau et al. 2004). These thematic maps were used in this study because they were observed in the field as the primary factors influencing landslides. The next step was to build and incorporate these parameters into our database (Fig. 3b). Various GIS procedures were applied, e.g., spatial interpolation to build the

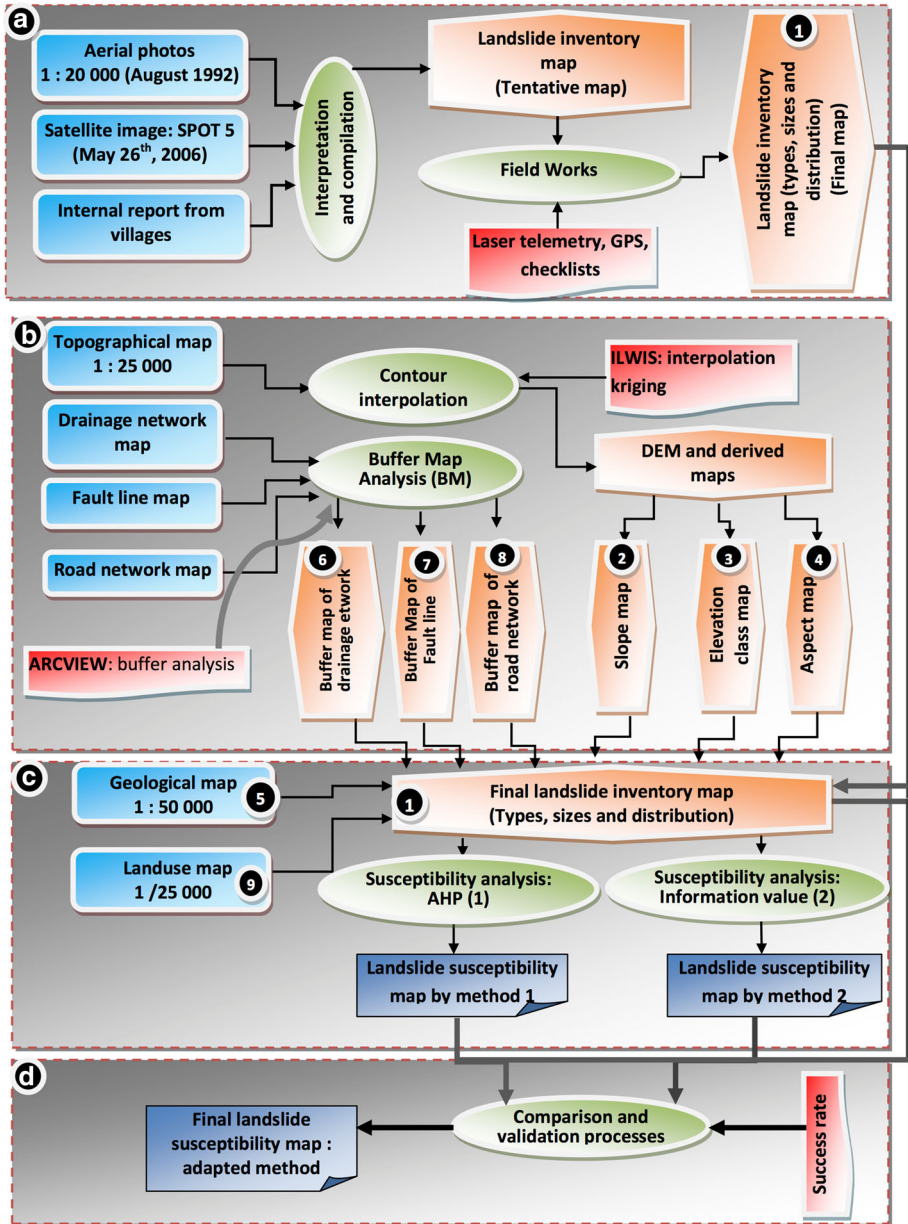


Fig. 3 Flowchart of research methodology

DEM and its derivative maps (slope map and aspect map); map overlaying and map calculation procedures to build landslide susceptibility map.

Topographic maps of scale 1 : 25,000 were used as base maps for mapping. All the thematic maps were then converted into raster formats. A Digital Elevation Model (DEM) (cell size: 5 m × 5 m) and its derivative maps (e.g., slope, aspect, and slope form) were

Table 1 Summary of data required for landslide susceptibility zonation

No.	Aims	Methods and data sources	Tools
I	Landslide inventory map	<ol style="list-style-type: none"> 1. Aerial photographs and SPOT image interpretation 2. Landslide report from local government, interview with local peoples 3. Fieldworks: landslide morphology and size measurement 	Stereoscopes, PC with ILWIS Camera, questionnaires Laster telemetry, GPS
II	DEM		
	Building parameter maps	<ol style="list-style-type: none"> 1. Contour interpolation by using kriging method from topographic map at 1: 25,000 scale 2. Cell size is 5 m × 5 m 	ILWIS
	Slope map	Derived from DEM by using “ <i>map calculation</i> ” module and classified by using “ <i>map slicing</i> ”	ILWIS
	Aspect map	Derived from DEM by using “ <i>map calculation</i> ” module and classified by using “ <i>map slicing</i> ”	ILWIS
	Slope form	Derived from DEM by using “ <i>filter operation</i> ” and classified by using “ <i>map slicing</i> ”	ILWIS
	Lithology	Digital geological map from Directorate of Geological Survey and checked by field work	ILWIS
	Buffer map of drainage network	<ol style="list-style-type: none"> 1. Digital topographic map at 1: 25,000 scale, 2. Map classification (<25, 25–50, 50–75, 75–100, 100–125, 125–150, >150 m) by using “<i>buffer analysis</i>” in ArcView 	ArcView and ILWIS
	Buffer map of fault line	<ol style="list-style-type: none"> 1. Digital geological map at 1: 25,000 scale 2. Map classification (<25, 25–50, 50–75, 75–100, 100–125, 125–150, >150 m) by using “<i>buffer analysis</i>” in ArcView 	ArcView and ILWIS
	Buffer map of road network	<ol style="list-style-type: none"> 1. Digital geological map at 1: 25,000 scale 2. Map classification (<25, 25–50, 50–75, 75–100, 100–125, 125–150, >150 m) by using “<i>buffer analysis</i>” in ArcView 	ArcView and ILWIS
	Land-use map	Digital topographic map at 1 : 25,000 scale, SPOT 5 image (13/05/2006)	ILWIS
III	Susceptibility analysis		
	Independency analysis	Cramers’ V independence test	SPSS
	Density analysis	Map crossing between landslide inventory map and parameter maps	ILWIS
		Analytical hierarchy process	ILWIS
	Susceptibility	Information value	ILWIS
IV	Comparison and validation		
	Map comparison	Map crossing and histogram analysis	ILWIS
	Validation	Success rate	ILWIS and Excel

developed from elevation data extracted from a 1:25,000 topographic map. These maps were then used to determine the influence of the terrain morphology on landslide occurrences. Derivative maps from DEM were developed in Integrated Land and Water Information System (ILWIS). The detail technique on developing the DEM and derivative

maps can be seen on ILWIS documentation (<ftp://ftp.itc.nl/pub/ilwis/ilwis30/pdf/chap10.pdf>).

The closeness of the slope to drainage, fault line, and road networks is also important factor for landslide susceptibility assessment. The closeness of the slope to drainage, fault line, and road networks is also an important factor for landslide susceptibility assessment. Drainage network control landslide occurrence by incision processes along the riverbank and saturation of the material along the river. Fault lines represent the weakened part of the rock formation and characterized by heavily fractured rocks. It triggers more weathering process since the fault line can be host of any stream water in long-term hydrologic process. Distance to the road is also important factor to landslides. Oversteeping along the road due to excavation process for road construction may increase the stress state to the slope and decrease the strength of the slope.

Buffer maps were therefore developed from three different raw maps (drainage network, road network, and fault line) to assess the influence of each distance of these maps onto landslide occurrence. Six classes of buffer zones were used with an interval distance of 25 m. The same interval of 25 m was chosen because the influences of the road, fault line, and drainage networks are maximum at that distance. The latter was due to the presence of cutting and filling for road construction and decrease with increasing interval distance. In addition, the same interval of 25 m was selected due to the pixel size of the map (5 m × 5 m). It would make easier for data handling. The lithological map was derived from the geological map (e.g., Rahardjo et al. 1995), whereas the land-use map was obtained from an Indonesian topographic map.

3.3 Conditional independence test

In order to ensure that the parameters controlling landslides are independent each other, a conditional independent test (Schicker and Moon 2012) was performed. The values of Chi-square (χ^2) were calculated to test the independency among parameters based upon pairwise comparison of all predictor parameters. In this case, landslide occurrence map was overlaid to all predictor parameters in order to extract the pixels as the samples for independent analysis. The value of Chi-square was then used as the input for determining the Cramer's V (Kendall and Stuart 1979; Van Den Eeckhout et al. 2006). The Cramer's V value was introduced to remove the effect of large sample size used in the analysis that probably causes a significant relationship (Thiery et al. 2007; Schicker and Moon 2012). The Cramer's V values vary from 0 to 1 with higher values reflecting a stronger association. In this study, the parameters were considered as dependent among them by the Cramer's value more than 0.5.

3.4 Landslide susceptibility assessment

Landslide susceptibility assessment was defined as determining the spatial probability of landslides through calculating the relation between the locations of past landslides and their influential factors, in order to predict the potential location of future landslides that have similar combinations of factors without considering the temporal probability (Van Westen et al. 2005). This susceptibility represents the spatial probability of landslides for a certain area. In this study, two different methods were applied: semiquantitative method by using analytical hierarchy process (AHP) and bivariate statistical approach by applying information value. As shown in Fig. 3c, the landslide inventory map must be analyzed with each parameter map separately, and this analysis must be repeated for all parameter maps

to determine their correlation and then build the landslide susceptibility index. Both of these methods were applied in this study for the following reasons: (1) the landslide susceptibility map resulted from AHP is based upon the expert opinion that is suitable for the area where the landslide data are absent, (2) AHP was applied to bridge between qualitative and quantitative approaches; (3) the bivariate statistical approach is relatively simple compared with the multivariate ones, since the bivariate statistical analysis incorporates one dependent variable and one independent variable. The importance of each variable to landslide is analyzed separately (Van Westen 1993). Simple map crossing can be done to conduct the bivariate method, while in the multivariate statistical analysis, multiple variables should be incorporated and analyzed simultaneously to determine the landslide susceptibility (Van Westen 1993). Bivariate statistical methods therefore can be applied to other areas in Indonesia more easily by governmental agencies, engineers, geoscientists, and decision makers.

3.4.1 Analytical hierarchy process (AHP)

To predict the location of future landslides, it is assumed that landslide occurrence is determined by landslide-related factors and that future landslides will occur under the similar conditions as previous landslides by assuming there is no extreme change from the present condition (Lee and Talib 2005). AHP can be used to determine the influence of landslide-related factor to the future landslides. AHP is one of methods comprising a multi-objective, multi-criteria decision-making approach to determine different alternatives of decisions (Saaty 1980; Saaty and Vargas 2001). AHP is widely used for many years on different applications in socioeconomic science, political science, and earth science. One of the most common uses of AHP is on landslide susceptibility zonation (e.g., Barredo et al. 2000; Castellanos Abella and Van Westen 2007, 2008; Yalcin and Bulut 2007; Yalcin 2008). This semiquantitative approach can be an alternative to bridge between qualitative and quantitative methods by evaluating the importance of parameters in the generation of landslide hazard maps (Van Westen et al. 2003; Hadmoko et al. 2010). AHP become one of the solutions for determining landslide susceptibility for the area that landslide data are very limited even unavailable. The proposed method was applied based upon the relative contribution of parameter maps to landslide occurrence that can be easily assessed. It makes more applicable in large region and developing countries like Indonesia (Hadmoko et al. 2010).

The AHP consists of five following steps: (a) determining the problems and break them down into structured component factors, (b) develop the hierarchy of component factors, (c) decide the value of each parameters to determine the relative contribution of each factor to landslide based upon expert judgment and experience and present them into a comparison matrix, (d) determine the normalized eigenvector representing the scores and weight of each factor to landslides, (e) conduct validation process by using the consistency ratio (CR) (Saaty and Vargas 2001; Pourghasemi et al. 2012; Kayastha et al. 2013). Relative contribution of parameter to landslides was determined by assigning the value between 1 and 9 (Table 2) in a pairwise comparison matrix.

The consistency ratio allows us to verify whether the assignment of relative contribution of parameters is consistent. The assessment can be acceptable the CR is lower than 0.1. The CR can be determined by using the following formula:

Table 2 Relative contribution of parameters in AHP (Saaty 1980)

Score of parameter	Degree of contribution	Description
1	Equally	Two factors contribute equally to the objective
3	Moderately	Experience and judgment slightly to moderately favor one factor over another
5	Strongly	Experience and judgment strongly favor one factor over another
7	Very strongly	The contribution of one factor is very strongly over another and its dominance is showed in practice
9	Extremely strong	The contribution of one factor is extremely strong over another and it presents the highest degree of affirmation
2, 4, 6, 8	Intermediate	Used to represent compromises between the preferences in weights 1, 3, 5, 7, and 9
Reciprocal	Opposites	Used for inverse comparison

$$CR = \frac{(\lambda_{\max} - n/n - 1)}{RI} \quad (1)$$

where λ_{\max} is the largest eigenvalue of the matrix that can be calculated from the matrix and n is the number of parameters used in the matrix. RI is the average of resulting consistency index depending on the order of the matrix (see Saaty 1980). Finally, the landslide susceptibility map can be determined by using the formula:

$$\begin{aligned} LSM = & (\text{Elevation} \times W_1) + (\text{Slope} \times W_2) + (\text{Aspect} \times W_3) + (\text{Slope morphology} \times W_4) \\ & + (\text{Geology} \times W_5) + (\text{Buffer of drainage networks} \times W_6) \\ & + (\text{Buffer of fault lines} \times W_7) + (\text{Buffer of road networks} \times W_8) \\ & + (\text{Landuse} \times W_9) \end{aligned} \quad (2)$$

where W_n is the weighted value of each parameter map.

3.4.2 Information value method

The information value method is a bivariate statistical method for spatial prediction of landslide event based on given parameter (Yin and Yan 1988; Jade and Sarkar 1993). Information value method was applied due its simplicity and become the solution when the variables introduced in landslide susceptibility assessment are combination of numerical variables and alphanumeric variables (Van Westen 1993). This combination is generally problematic in statistical analysis. This can be solved by using two binary variables such as the presence (1) and absence of landslide (0). The basic principle of this method is that the landslide susceptibility depends on the spatial density that can be considered as spatial probability of landslide event on specified parameter map. Landslide susceptibility map was resulted from relationship between the spatial distribution of landslide events and parameter map. The information value is the product of log natural of the landslide density of each parameter map used. The formula used for calculating susceptibility is as follows:

$$IV = \ln \frac{L_i/L}{A_i/A} \quad (3)$$

L_i is the area of parameter class i covered by landslides; L is the area of landslides for the entire area; A_i is the area of the parameter class i ; A is the area of Kayangan Catchment (35.5 km²).

The susceptibility index (S) can be calculated using the following formula:

$$S = \sum_{j=1}^{j=n} IV_{ij} \quad (4)$$

IV_{ij} is the information value of variable i for parameter j ; n is the number of variables.

In some cases, the areas having no landslide provides undefined value (∞) of the log natural; therefore, the result has to be assigned to zero (Yalcin 2007).

3.4.3 Map validation

The map validation was the comparison between the resultant map and the independent landslide inventory map for 2009. Several methods of map validation have been used by scientists, from qualitative or visual methods to a simple quantitative method of calculating the area covered by landslides for every susceptibility level to a complex method using success rate curves (Remondo et al. 2003; Chung et al. 1995; Hadmoko 2009).

Success rate can be determined by calculating the area under the curve (AUC) from the number of pixels of the susceptibility map in a certain number of classes, from the high values to the low values (on the x -axis), based on the histogram with the corresponding number of landslides (on the y -axis). The x -axis represents the cumulative surface of the susceptibility index, and the y -axis represents the cumulative surface of landslides of each portion of the susceptibility index (Remondo et al. 2003).

4 Results

4.1 Spatial distribution of landslides

A total of 131 and 49 landslides were inventoried for the entire area of Kayangan Catchment for the periods of 2007–2008 and 2009, respectively (Fig. 4). They are primarily distributed in the upper and middle parts of the study area due to the very rough topographic comprising gentle to very steep slope. The absence of landslide events across the lower catchment is due to the flat terrain, which is dominated by alluvial plain and river terraces. The landslide surface area for the entire catchment is 0.127 km², with a landslide density of 4.21 events/km² and a landslide area density of 4×10^{-3} km²/km². All landslides in the study area were considered to be shallow landslides, with average landslide depth 3 m and an average surface area of 968 m² (Hadmoko et al. 2009).

Five types of landslides were identified: creep, flow, fall, slide, and slump. The majority of the landslides in this area were slides, followed by slumps, creeps, and flows, with a frequency of 94, 26, 4, and 4, respectively. Only two rockfalls were identified in this area. Slides are translational in nature because the sliding surface is relatively shallow that lessening the possibility of circular movement of the material.

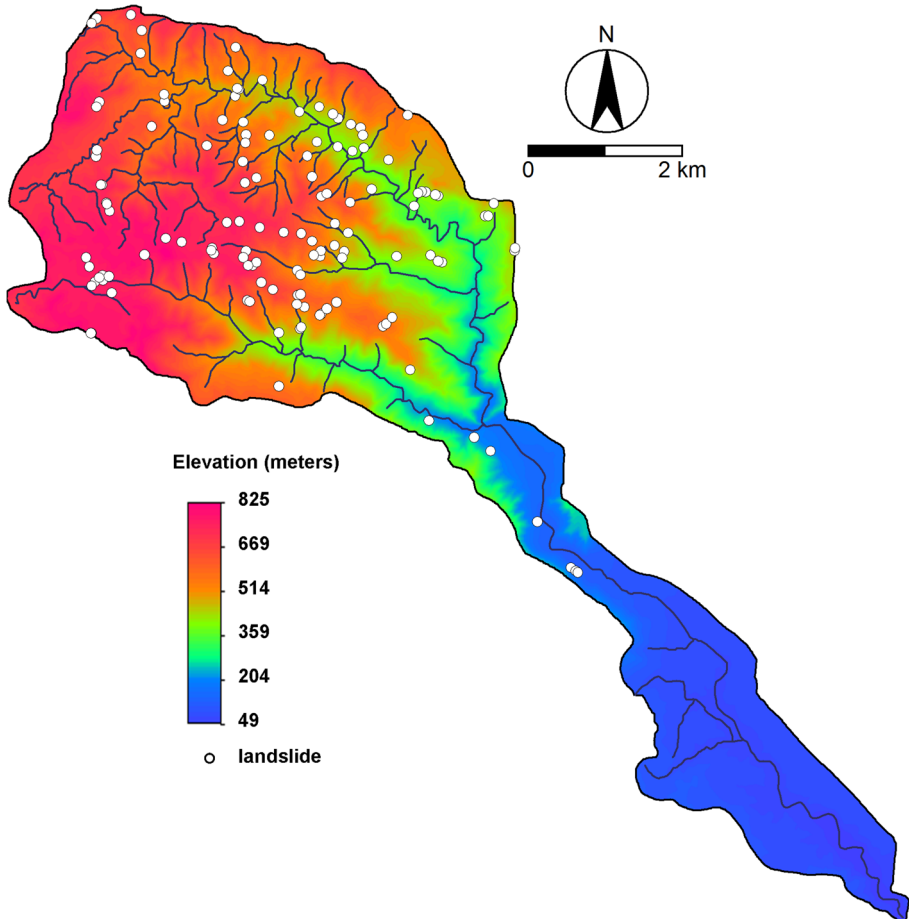


Fig. 4 Landslide distribution and DEM in Kayangan Catchment

The majority of landslides are characterized by the high clay content with high soil moisture or even saturated conditions. The presence of water plays an important role in the triggering of landslides by increasing both the weight of the saturated soil and the pore water pressure. A summary of landslide spatial distribution and its correlation with terrain parameters was completed by Hadmoko et al. (2009).

4.2 Parameter maps

4.2.1 Elevation class map and slope map

Overlaying the landslide inventory map over the elevation map illustrates landslide occurrence with increasing elevation, up to 500 m (Fig. 5a). In contrast, above 500 m, landslide events tended to decrease in frequency with increasing elevation, until 700 m. The landslide decreasing activity in the upland slopes is due to the presence of more resistant lithology, such as andesitic breccias, whereas the middle of the catchment was

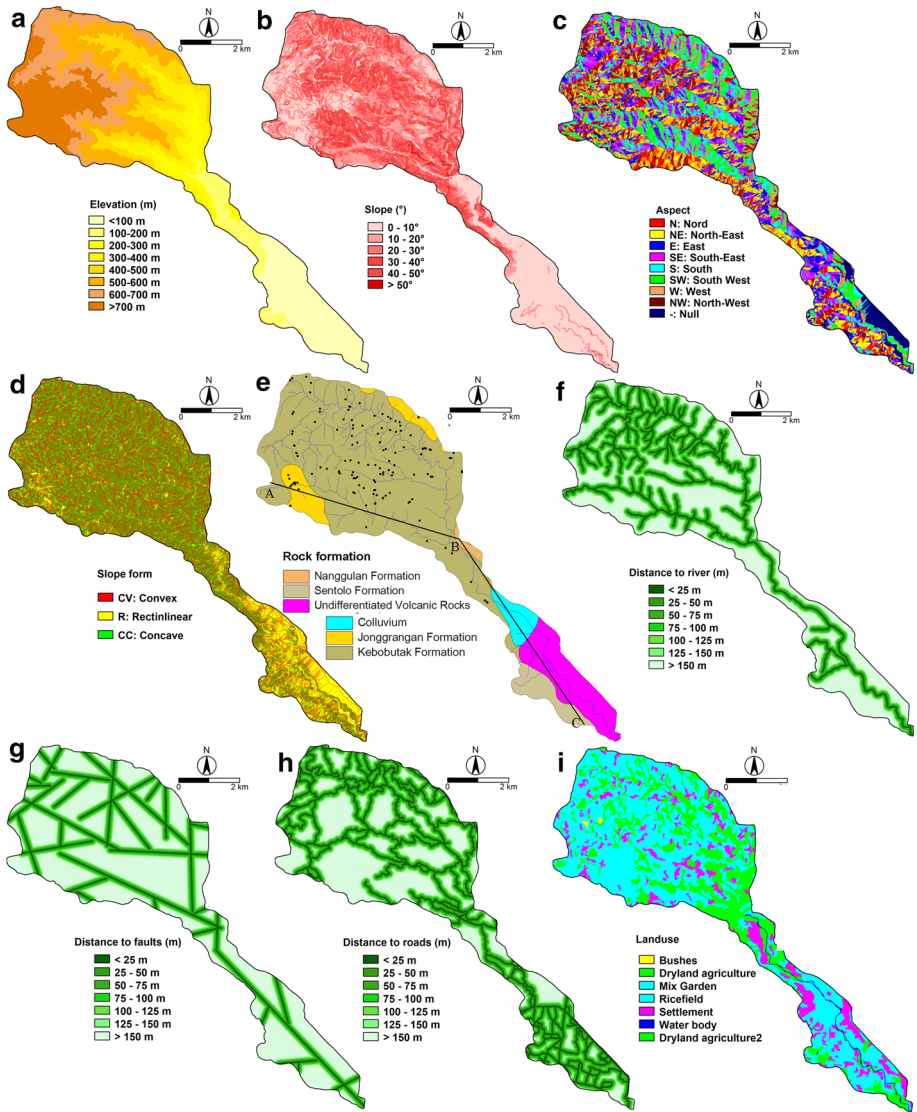


Fig. 5 Landslides and parameter maps: **a** elevation; **b** slope; **c** aspect; **d** form; **e** lithology; **f** buffer of drainage network; **g** buffer of fault line; **h** buffer of road network; and **i** land use

covered by unconsolidated materials such as colluviums, which are regularly subjected to landslides (Rahardjo et al. 1995).

4.2.2 Slope map

The relationship between landslide occurrence and slope shows that higher landslide frequency occurred on steeper slopes up to a slope steepness of 20°–30°, and thereafter the frequency decreased with increasing slope angle (Fig. 5b). The highest density of

landslides both in terms of number and area was found on the steepness ranging from 20° to 30° (0.047 events/km² and 7/1000 km²). However, an inverse correlation with landslide events occurs with slope steepness greater than 30°, when the landslide frequency decreases with increasing slope angle. This phenomenon is closely related to the influence of other factors such as lithology and human activities. Slopes with greater than 30° are generally carved in resistant rock (Rahardjo et al. 1995), on which the weathered materials are relatively shallow or even absent. In addition, human activities on very steep slopes exist, but they are less common than on less steep slopes.

4.2.3 Aspect map

The aspect of a slope can influence landslide initiation because it affects the path of sun during the day time, moisture retention and vegetation cover and, in turn, soil strength and susceptibility to landslides. The amount of rainfall on a slope may also vary depending on its aspect, especially in hilly and mountainous areas, due to the impact of orographic rainfall (Fig. 5c). Most landslide events were concentrated in the NE, E, SE, and S directions compared with other orientations, which could be caused by the amount of rainfall, humidity, and solar radiation, which influence landslide activity. Overlaying the slope and orientation maps showed that the NE, E, SE, and S orientations had steeper slope inclinations.

4.2.4 Slope profile

Slope profile was used to detect which part of the slope is convex, concave, or rectilinear in both *x*- and *y*-directions. It was developed by using the second derivative of filter operation applied to DEM in ILWIS. The lower curvature (convex), medium curvature (rectilinear), and upper curvature (concave) are presented by the value of derivative DEM such as <0.5; −0.5 to 0.5; and >0.5, respectively (<ftp://ftp.itc.nl/pub/ilwis/ilwis30/pdf/chap10.pdf>).

Landslides were more abundant on concave (65 events) and convex (55 events) slopes, whereas these phenomena were less common on rectilinear slopes (13 events), where the landslide density was also less (Fig. 5d). These data demonstrated that the convex and concave slopes were more susceptible to landslides. Slope profiles (concave, convex, and rectilinear) can have significantly different susceptibility to landslide. The forms control the driving and resisting forces within the direction of landslide and the convergence or divergence of landslide material and water in the direction of landslide motion (Carson and Kirkby 1972; Ohlmacher 2007). Concave and convex slopes are usually distributed on steeper terrains. They are associated with spurs and gullies, which were developed by erosion and landslide process. The rectilinear slopes are generally associated with gentle slope or even flat terrain, which were found in the lower catchment in this study area. Concave slopes retain more precipitation through infiltration, which increases pore water pressure.

4.2.5 Lithological map

The analysis of landslide activities and geological formations showed that only two lithologies were subject to landslides: the Kebobutak Formation and the Jonggrangan Formation. Most landslides occurred in the Kebobutak Formation (119 events), followed by the Jonggrangan Formation (Fig. 5e). Most of the landslides occurred in the Kebobutak

Formation due to the extreme weathering and fracturing of the andesite and andesitic breccias that played an important role in the predisposition to landslides. Twelve landslides were also identified in the Jonggrangan Formation, mostly in calcareous sandstone and limestone. Landslides were absent in other types of rocks because those lithologies are situated at the southern and eastern parts of Kayangan Catchment with flat and gentle terrain.

4.2.6 Buffer zone of drainage network

The analysis of the relationship between landslide frequency and the stream network buffer zone revealed that most landslides occurred less than 150 m from rivers (46 events, or 3.46 events/km²) (Hadmoko et al. 2009) (Fig. 5f). Only 14 landslides occurred on the zone with the distance less than 25 m from rivers. There was no decrease in landslide frequency with increasing distance from rivers. However, the area of landslides was greatest within the buffer zone, less than 25 m from a river, indicating that most large landslides were situated near rivers due to the slope modification of gully erosion and river undercutting of slope toes, which influences the initiation of landslides.

4.2.7 Buffer zone of fault line

The analysis of the relation between slope instability and the fault line buffer zones indicated that the number and the area of landslides decreased slightly as the distance from the fault line increased from 0 to 150 m, then increased abruptly beginning at 150 m from the fault line (Fig. 5g). Fault lines in Kayangan Catchment are generally associated with an abrupt change in topography or an escarpment with near-vertical slopes. The presence of a fault can fracture rock materials and decrease their stability. The area and number of landslides decreased slightly with increasing distances from faults, indicating that landslide occurrence was not always associated with the existence of the faults.

4.2.8 Buffer zone of road network

The road construction significantly decreases the slope stability of the hilly area and accelerate landslide occurrence (Khan and Lateh 2011; Das et al. 2012). We analyzed landslide frequency at varying distances from road networks to determine the contribution of anthropogenic slope cuts to landslide occurrences (Fig. 5h). Most landslides occurred in the zone closest to road networks (<25 m), with 83 landslide events (63% of total landslides) mapped in this area and with number and area densities of 36.55 events/km² and 28 km²/km², respectively. In general, landslide frequency decreased with increasing distance from the road. This trend reveals that road networks play an important role in landslide initiation due to the increase in the microtopography created during the slope cutting. The landslides were well spread both above the road due to the cutting impacts and below the road as the consequence of unconsolidated filled materials. Human activities of this type have initiated and accelerated landsliding in this region, particularly via undercutting and the removal of material from the toe of slopes to build roads (Fig. 6a).

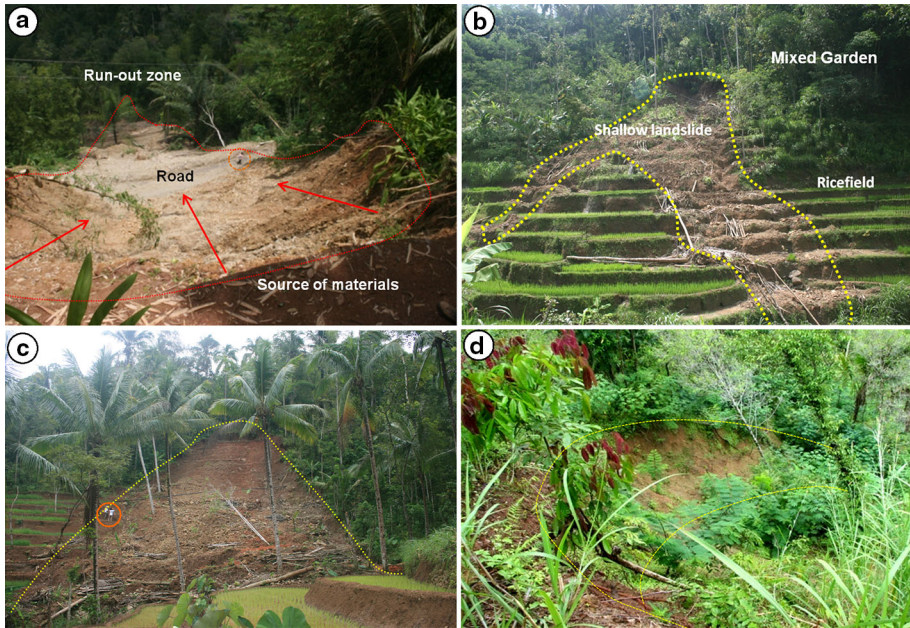


Fig. 6 Landslides at the study area: **a** translational landslide occurred on steep slope due to cutting and filling for road reconstruction, **b**, **c** landslides on agricultural land and mixed garden due to the presence of rice field causing continuous soil saturation and **d** rotational landslide occurred on mixed garden which occurred near the settlement areas

4.2.9 Land-use map

The analysis of landslide occurrence based on land use showed that landslides occurred only in three types of land use: mixed garden, settlement, and agricultural area (Figs. 5i, 6b, c). Mixed garden is the land use most exposed to landslides (72 events) (Fig. 6b, d), with number and area densities of 4.06 events/km² and 6.2/1000 km², respectively. However, the highest number and area densities of landslides were identified for the settlement land-use class, with values of 11.028 events/km² and 10.8/1000 km², respectively. The spatial distribution of landslides on most manmade terrains (e.g., settlements and roads via slope cutting) underlines the human contribution to landslide triggering (Fig. 7). In contrast, natural slopes that are densely covered by vegetation tend to reduce the action of climatic agents such as rain, thereby preventing erosion due to the natural anchorage provided by the tree roots; thus, they are less prone to landslides.

4.3 Susceptibility analysis

4.3.1 Testing of conditional independence

Result of Chi-square test confirms an independent relation among the predictor parameters containing landslides with the significant level: 0.01. Table 3 summarizes the result of Chi-square analysis through the Cramer V value for all parameters. The Cramer V is relatively low with the value vary from 0.08 to 0.42, and there is no value higher than 0.5 found on

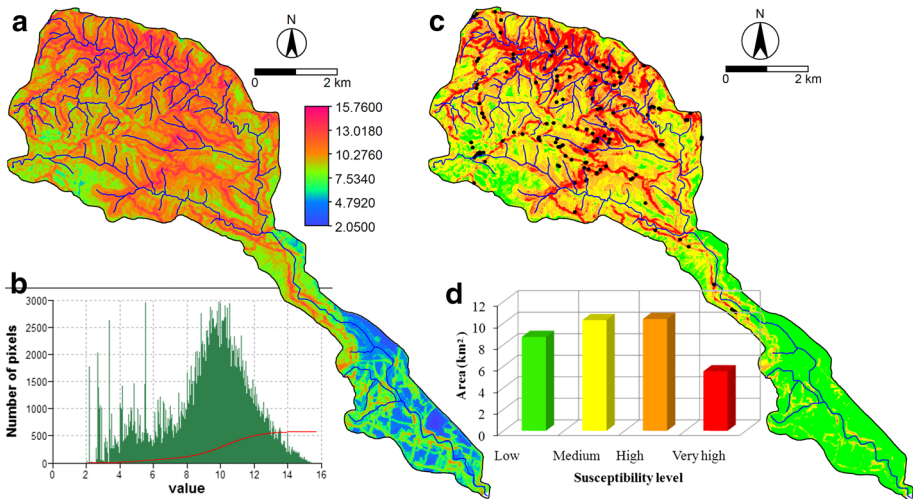


Fig. 7 Result of landslide susceptibility assessment by AHP method: **a** raw spatial landslide susceptibility map; **b** histogram showing the landslide susceptibility index; **c** final landslide susceptibility map; and **d** histogram of final landslide susceptibility index value

the result. Therefore, all parameters are conditionally independent and can be used as predictor parameters for determining the landslide susceptibility.

4.3.2 AHP

The AHP analysis (Table 4) resulted equation of weighted parameters to determine landslide susceptibility map as follows:

$$\begin{aligned}
 \text{LSM} = & (\text{Elevation} \times 0.1749) + (\text{Slope} \times 0.2176) + (\text{Aspect} \times 0.0916) \\
 & + (\text{Slope morphology} \times 0.0956) + (\text{Geology} \times 0.1497) \\
 & + (\text{Buffer of drainage networks} \times 0.0602) + (\text{Buffer of fault lines} \times 0.0335) \\
 & + (\text{Buffer of road networks} \times 0.1141) + (\text{Landuse} \times 0.0629).
 \end{aligned}$$

Among the nine parameters introduced to the equation, slopes became the most important parameter to landslides (0.24) followed by geology (0.136), buffer of road network (0.134), and elevation (0.13). The lowest contribution parameter to landslide susceptibility was buffer to fault line (0.037) followed by buffer to drainage network (0.071). The analysis was considered as consistent since the CR was less than 0.1 (CR = 0.089). These values indicated that slope played an important role on landslide occurrence. Slopes contributed on gravitational force that facilitated the down movement of materials from the upper slopes. Geology was also assigned as important factor to landslide occurrence because of the presence of intensively weathered tertiary volcanic materials. The incised and fully weathered volcanic rocks made the rainwater infiltrate and percolate more easily through cracks and joints. Road network was considered as one of the most important factors to landslides after slope and geology due to the high occurrence of landslides on road corridor.

As observed in Table 5, the weight value of elevation was highest at the class of 500–600 m (0.2178) and tended to decrease by increasing the elevation. The latter is

Table 3 Crosstab of Cramer's V value for calculating the Chi-square contingency tables

	Elevation	Slope	Slope aspect	Slope morphology	Geology	Buffer of drainage network	Buffer of fault lines	Buffer of road networks	Land use
Elevation									
Slope	0.204								
Slope aspect	0.252	0.161							
Slope morphology	0.08	0.072	0.118						
Geology	0.420	0.226	0.217	0.076					
Buffer of drainage network	0.225	0.114	0.112	0.089	0.127				
Buffer of fault lines	0.257	0.077	0.210	0.049	0.211	0.143			
Buffer of road networks	0.160	0.083	0.143	0.045	0.098	0.144	0.163		
Land use	0.230	0.202	0.147	0.033	0.263	0.313	0.192	0.167	

Table 4 Weighting result of AHP method of parameters

Parameters	Code	P1	P2	P3	P4	P5	P6	P7	P8	P9	Weight
Elevation	P1	1	1/3	2	3	1/2	2	4	1/2	3	0.130
Slope	P2	3	1	3	3	2	3	5	2	4	0.240
Aspect	P3	1/2	1/3	1	1	1/2	2	4	1/2	2	0.092
Slope morphology	P4	1/3	1/3	1	1	1/2	2	3	1/2	2	0.086
Geology	P5	2	1/2	2	2	1	1	3	2	1/2	0.136
Buffer of drainage networks	P6	1/2	1/3	1/2	1/2	1	1	2	1/3	2	0.071
Buffer of fault lines	P7	1/4	1/5	1/4	1/3	1/3	1/2	1	1/3	1	0.037
Buffer of road networks	P8	2	1/2	2	2	1/2	3	3	1	1	0.134
Land use	P9	1/3	1/4	1/2	1/2	2	1/2	1	1	1	0.075

Consistency ratio = 0.089

associated with the geomorphological characteristic of study area. The higher part of the study area (>600 mm a.s.l.) is a part of the plateau that is characterized by gentle terrain; therefore, the landslide occurrence tended to decrease. The weight value of slope increased with increase in steepness. It means that more slope steep, more landslide to likely occur.

Slopes facing to the S, SE, E, and NE had higher weight factors compared with the other slope aspects because south-facing slopes receive more rainfall than north-facing slopes since the south to east facing is the concentration of the condensation process due to orographic effect. Slope aspect controls evapotranspiration and the amount of water trapped by slopes through orographic rainfall. Soil moisture content controls pore water pressure, which has a great influence on slope stability. In addition, the slope orientation controls the ratio between the infiltration and runoff ratio especially for the uncovered soil at the beginning of the crop cycle.

Concave and convex slope morphologies had a great influence on weight values because the quantity of water trapped by concave and convex slopes is much greater than that trapped by rectilinear slopes. Concave and Convex slope trap the same quantity of water. Concave slopes tend to have high water infiltration as a consequence of the existence of a depression.

Only two lithological formations resulted in the high influence to landslide susceptibility: the Kebobutak formation and the Jonggrangan formation. These two formations consist of highly weathered, unstable, and pulverized, which could be due to the presence of faults in that area. In addition, the presence of cracks and joints contributes significantly on lessening the slope stability due to the acceleration of infiltration process.

The analysis showed that the weight value decreased significantly with increasing distance from a road. The distance to a fault line had no clear effect on weight value, indicating that fault lines had a low influence on landslide occurrences.

The susceptibility assessment through the AHP resulted in the susceptibility index map (Fig. 7a) and the histogram of total scores, ranging from 0.093 to 0.669 (Fig. 7b). Figure 7b shows the pixel value distribution based on the total scores of the 9 parameters that were introduced during the susceptibility assessment. Through this histogram, the final susceptibility map was created through the module “MapSlicing” in the Integrated Land and Water Information System (ILWIS) environment, a raster-based GIS developed by ITC, the Netherlands. We classified the susceptibility level into four classes: low, medium,

Table 5 Pairwise comparison matrix and normalized principal eigenvector resulted from AHP

Parameter	No.	Values/classes	1	2	3	4	5	6	7	8	9	Weight
Elevation	1	<100	1	1/2	1/3	1/4	1/4	1/5	1/5	1/5	1/5	0.0318
	2	100–200	2	1	1/2	1/3	1/4	1/5	1/5	1/4	1/4	0.0420
	3	200–300	3	2	1	1/2	1/3	1/4	1/4	1/3	1/3	0.0629
	4	300–400	4	3	2	1	1/2	1/3	1/3	1/3	1/3	0.0913
	5	400–500	4	4	3	2	1	1/2	1	1/2	1/2	0.1473
	6	500–600	5	5	4	3	2	1	1	1	1	0.2178
	7	600–700	5	5	4	3	1	1	1	1	1	0.2008
	8	>700	5	4	3	3	2	1	1	1	1	0.2057
Consistency ratio = 0.033												
Slope	1	0–10	1	1/3	1/4	1/4	1/5	1/5				0.2596
	2	Oct-20	3	1	1/2	1/3	1/4	1/3				0.4987
	3	20–30	4	2	1	1/2	1/3	1/3				0.7337
	4	30–40	4	3	2	1	1/2	1/2				1.1196
	5	40–50	5	4	3	2	1	1/2				1.6712
	6	>50	5	3	3	2	2	1				2.010
Consistency ratio = 0.061												
Aspect	1	N	1	1/2	1/2	1/3	1/2	1/2	1/3	1/2	5	0.0666
	2	NE	2	1	1	2	1/2	2	2	2	4	0.1536
	3	E	2	1	1	1	1	2	2	3	4	0.1537
	4	SE	3	1/2	1	1	1	2	3	3	4	0.1611
	5	S	2	2	1	1	1	3	2	2	4	0.1726
	6	SW	2	1/2	1/2	1/2	1/3	1	1	3	3	0.0932
	7	W	3	1/2	1/2	1/3	1/2	1	1	2	4	0.0969
	8	NW	2	1/2	1/3	1/3	1/2	1/3	1/2	1	5	0.0733
	9	Flat	1/5	1/4	1/4	1/4	1/4	1/3	1/4	1/5	1	0.029
Consistency ratio = 0.077												
Slope morphology	1	Concave	1	3	1							0.4429
	2	Rectilinear	1/3	1	1/2							0.1699
	3	Convex	1	2	1							0.3873
Consistency ratio = 0.0216												
Geology	1	Kebobutak	1	1	3	3	3	2	1	1	3	0.283
	2	Jonggrangan	1	1	3	3	3	2	1	1	3	0.283
	3	Colluvium	1/3	1/3	1	1	1	1/2	1/3	1/3	1	0.090
	4	Nanggulan	1/3	1/3	1	1	1	1/2	1/3	1/3	1	0.090
	5	Sentolo	1/3	1/3	1	1	1	1/2	1/3	1/3	1	0.090
	6	Volcanic rock	1/2	1/2	2	2	2	1	1/2	1/2	2	0.164
Consistency ratio = 0.003												

Table 5 continued

Parameter	No.	Values/classes	1	2	3	4	5	6	7	8	9	Weight
Buffer of drainage networks	1	<25	1	3	3	4	5	5	6			0.3639
	2	25–50	1/3	1	2	3	3	5	5			0.2154
	3	50–75	1/3	1/2	1	3	2	4	3			0.1533
	4	75–100	1/4	1/3	1/3	1	1	3	4			0.0966
	5	100–125	1/5	1/3	1/2	1	1	2	3			0.0840
	6	125–150	1/5	1/5	1/4	1/3	1/2	1	2			0.0497
	7	>150	1/6	1/5	1/3	1/4	1/3	1/2	1			0.0371
		Consistency ratio = 0.0693										
Buffer of fault lines	1	<25	1	1	2	3	5	6	6			0.3021
	2	25–50	1	1	1	2	4	5	5			0.2387
	3	50–75	1/2	1	1	1	3	4	3			0.1704
	4	75–100	1/3	1/2	1	1	3	3	2			0.1322
	5	100–125	1/5	1/4	1/3	1/3	1	1	2			0.06023
	6	125–150	1/6	1/5	1/4	1/3	1	1	1			0.0480
	7	>150	1/6	1/5	1/3	1/2	1/2	1	1			0.04878
		Consistency ratio = 0.019										
Buffer of road networks	1	<25	1	2	3	5	6	7	7			0.3558
	2	25–50	1/2	1	2	4	5	6	7			0.2497
	3	50–75	1/3	1/2	1	3	4	5	5			0.1698
	4	75–100	1/5	1/4	1/3	1	3	3	4			0.0958
	5	100–125	1/6	1/5	1/4	1/3	1	2	3			0.0585
	6	125–150	1/7	1/6	1/5	1/3	1/2	1	2			0.0406
	7	>150	1/7	1/7	1/5	1/4	1/3	1/2	1			0.03
		Consistency ratio = 0.074										
Land use	1	Dryland agriculture	1	1/2	1/2	1/2	3	3				0.2070
	2	Mix garden	2	1	1/2	1/2	4	4				0.2890
	3	Settlement	2	2	1	1	5	5				0.4233
	4	Bushes	2	2	1	1	5	5				0.4233
	5	Rice fields	1/3	1/4	1/5	1/5	1	1				0.0767
	6	Water bodies	1/3	1/4	1/5	1/5	1	1				0.0767
		Consistency ratio = 0.025										

high, and very high (Fig. 7c). The final susceptibility map shows that Kayangan Catchment was dominated by high susceptibility areas (10.6 km²), followed by moderate susceptibility areas (9.08 km²). Only 6.49 km² of the study area was considered to be very highly susceptible (Fig. 7d).

Visual interpretation of the landslide susceptibility map by the AHP shows that most of the very high and high susceptibility zones were widely distributed in the upper and middle areas of Kayangan Catchment. The pattern of very high susceptibility zones indicates the dominant influence of slopes on landslide susceptibility. The middle and lower susceptibility levels are broadly spread across the middle of the catchment and cover most of the lower part of Kayangan Catchment.

4.3.3 Information value

The information value method was also applied to assess landslide susceptibility. Weight values for each parameter were introduced during the analysis that ranged from -2.224 to 1.070 (Table 6). The minimum weight value was for the 100–200-m elevation class, whereas the maximum value was for a road distance less than 25 m. Negative value indicated that a given parameter was unfavorable to landslide susceptibility, and in contrast, the positive value signified that this parameter was favorable to landslide susceptibility. A value of zero had no influence on landslide occurrence.

The most favorable elevation class for landslides was up to 500 m, whereas elevations of 100–400 m or those greater than 700 m had negative influences on landslide occurrence. Elevations less than 100 m had no influence on landslide occurrence. Slope angles of 10° – 30° increased landslide frequency, whereas those greater than 30° or less than 10° had negative influences on landslide occurrence.

Slopes facing to the NE, E, SE, and S were favorable to landslide occurrence, represented by positive values, whereas the other aspects had a negative influence on landslide occurrence. Concave and convex slope forms had positive values, whereas linear forms had negative weight values. This trend appears similar to that of the frequency ratio method. Most buffer zones for hydrologic networks had positive weight values, except for the zone greater than 150 m from the drainage network. This trend indicates that the drainage network had a favorable influence on landslide occurrence.

The role of human influence in landslide susceptibility was represented by the buffer zone of the road network and land-use type. Only two classes of road networks were favorable to landslides: the zone less than 25 m from roads and the zone 25–50 m from roads. The zones greater than 50 m from the road network were unfavorable to landslides. Among the land-use types, dryland agriculture, mixed garden, and settlements were favorable to landslide occurrence, whereas the others had no influence on slope failure. These phenomena suggest that human activities are an important influence aggravating landslide hazard in Kayangan Catchment.

Overlaying all the parameter maps (V1–V9) together resulted in the raw susceptibility index map (Fig. 8a) that represents the total weight, with values ranging from -7.81 to 4.67 (Fig. 8b). Raw data classification was performed to build the final susceptibility map (Fig. 8c) through histogram classification. Kayangan Catchment is divided into four susceptibility classes: low, medium, high, and very high (Fig. 8d). Based on the analysis of the attribute data, it can be stated that the areas of low, medium, high, and very high susceptibility were 8.71, 9.42, 10.74, and 6.04 km², respectively.

Upon examining the spatial pattern of landslide susceptibility (Fig. 8d), the very high and high susceptibility zones were widely distributed in the northeastern part of Kayangan Catchment, which is the upper part of this drainage basin. These zones of high susceptibility were generally associated with the drainage network and the road network. This pattern was closely related to weight values of the stream network and the road network, as previously discussed. The medium susceptibility zone covers the northwestern and central parts of Kayangan Catchment, which were generally associated with the zone situated less than 150 m from the river network. The low susceptibility area was distributed on the plain and gentle slopes, primarily in the lower or southern part of Kayangan Catchment or the western part of Kayangan Catchment.

Table 6 Weighting result of information value method

Parameter	Values/classes	Class area (km ²)	Landslide area (km ²)	% Landslide area	% Class area	IV
Elevation	<100	6.05	0	0.00	17.04	0.000
	100–200	2.57	0.001	0.79	7.24	−2.224
	200–300	1.85	0.004	3.15	5.21	−0.509
	300–400	3.27	0.006	4.72	9.21	−0.674
	400–500	4.81	0.033	25.98	13.55	0.645
	500–600	5.92	0.046	36.22	16.68	0.770
	600–700	5.24	0.021	16.54	14.76	0.108
	>700	5.58	0.016	12.60	15.72	−0.227
Slope	0–10	10.7	0.012	9.45	30.14	−1.166
	10–20	7.57	0.038	29.92	21.32	0.333
	20–30	8.21	0.047	37.01	23.13	0.464
	30–40	6.01	0.021	16.54	16.93	−0.029
	40–50	2.13	0.007	5.51	6.00	−0.091
	>50	0.66	0.001	0.79	1.86	−0.865
Aspect	N	3.96	0.006	4.72	11.15	−0.865
	NE	6.19	0.03	23.62	17.44	0.298
	E	5.24	0.025	19.69	14.76	0.282
	SE	4.64	0.019	14.96	13.07	0.129
	S	4.34	0.023	18.11	12.23	0.387
	SW	4.16	0.011	8.66	11.72	−0.308
	W	2.6	0.007	5.51	7.32	−0.290
	NW	2.38	0.005	3.94	6.70	−0.538
	Flat	1.77	0	0.00	4.99	0.000
Slope morphology	Concave	13.3	0.062	48.82	37.46	0.259
	Rectilinear	7.06	0.013	10.24	19.89	−0.670
	Convex	14.66	0.053	41.73	41.30	0.005
Geology	Kebobutak	25.83	0.12	94.49	72.76	0.255
	Jonggrangan	2.15	0.006	4.72	6.06	−0.254
	Colluvium	1.22	0	0.00	3.44	0.000
	Nanggulan	0.3	0	0.00	0.85	0.000
	Sentolo	1.64	0	0.00	4.62	0.000
	Volcanic rock	4.1	0	0.00	11.55	0.000
Buffer of drainage networks	<25	4.25	0.026	20.47	11.97	0.538
	25–50	4.11	0.016	12.60	11.58	0.086
	50–75	3.85	0.019	14.96	10.85	0.323
	75–100	3.51	0.018	14.17	9.89	0.362
	100–125	3.14	0.018	14.17	8.85	0.473
	125–150	2.76	0.016	12.60	7.77	0.484
	>150	13.65	0.013	10.24	38.45	−1.322

Table 6 continued

Parameter	Values/classes	Class area (km ²)	Landslide area (km ²)	% Landslide area	% Class area	IV
Buffer of fault lines	<25	3.02	0.013	10.24	8.51	0.186
	25–50	2.98	0.013	10.24	8.39	0.200
	50–75	2.85	0.011	8.66	8.03	0.077
	75–100	2.67	0.011	8.66	7.52	0.143
	100–125	2.56	0.008	6.30	7.21	−0.134
	125–150	2.36	0.007	5.51	6.65	−0.186
	>150	18.85	0.064	50.39	53.10	−0.051
Buffer of road networks	<25	6.05	0.063	49.61	17.04	1.070
	25–50	5.21	0.025	19.69	14.68	0.295
	50–75	4.38	0.01	7.87	12.34	−0.448
	75–100	3.61	0.009	7.09	10.17	−0.360
	100–125	2.92	0.008	6.30	8.23	−0.265
	125–150	2.31	0.006	4.72	6.51	−0.319
	>150	10.8	0.005	3.94	30.42	−2.043
Land use	Dryland agriculture	9.41	0.057	44.88	26.51	0.528
	Mix garden	17.75	0.111	87.40	50.00	0.560
	Settlement	4.52	0.035	27.56	12.73	0.774
	Bushes	0.05	0	0.00	0.14	0.000
	Rice fields	3.27	0	0.00	9.21	0.000
	Water bodies	0.28	0	0.00	0.79	0.000

5 Discussion

In this study, two landslide susceptibility maps were conducted. These maps were developed through a analytical hierarchy process (AHP) and information value method. In the previous section, these two results were verified, validated, and compared to choose the most appropriate model for the study area. Many previous studies have been conducted to compare and validate landslide susceptibility maps (e.g., Carrara 1983; Brabb 1984; Yin and Yan 1988; Duque et al. 1991; Mulder 1991; Carrara et al. 1991, 1995; Van Westen 1993; Chung et al. 1995; Irigaray et al. 1996, 1999; Chung and Fabbri 1998, 1999; Dhakal et al. 1999; Remondo et al. 2003; Hadmoko et al. 2010; Pourghasemi et al. 2012; Kayastha et al. 2013). They assumed that future slope failures would be more likely to occur under those conditions that caused past and present instability. Hence, future landslides would occur under conditions and factors equal or similar to those for comparable past landslides, such as slope, geology, soil, and land use. Therefore, the final susceptibility map was validated based on this previous assumption. The landslide susceptibility map is then valid if the majority of the present and past landslides occurred within the zone considered to be susceptible.

The AHP model had a prediction accuracy of 80%, whereas the information value model had an accuracy of 83% (Fig. 9). The accuracy of the information value model was better than that of the AHP. In the AHP model, the most susceptible 10% of the area explained 25% of all of the landslides, and the most susceptible 20% of the area contained

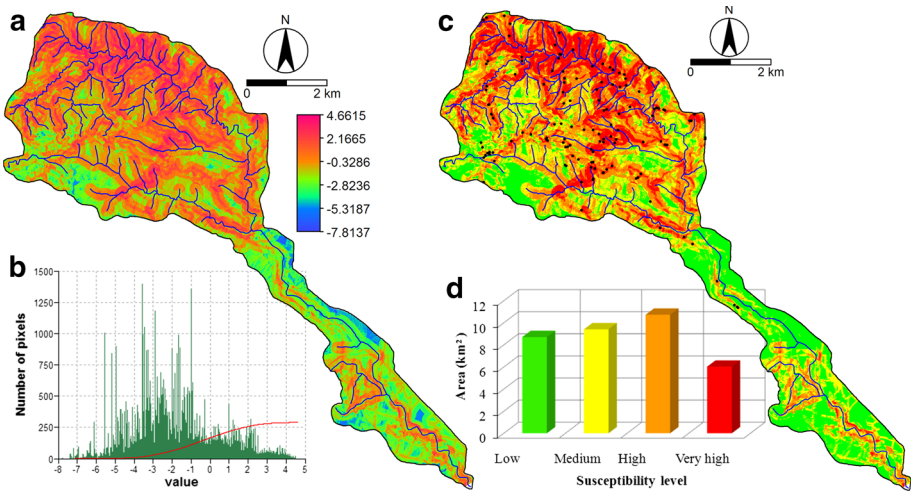


Fig. 8 Result of landslide susceptibility assessment by information value method: **a** raw spatial landslide susceptibility map; **b** histogram showing the landslide susceptibility index; **c** final landslide susceptibility map; and **d** histogram of final landslide susceptibility index value

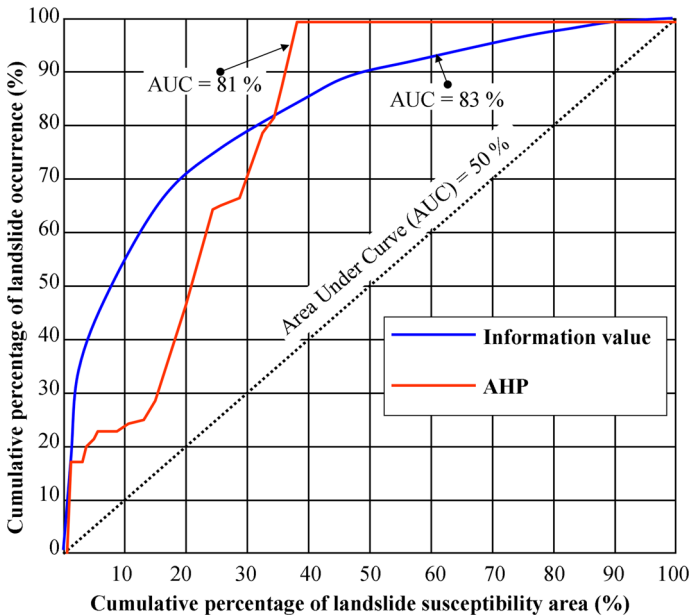


Fig. 9 Success rate of landslide susceptibility maps

26% of the total landslides. In the information value model, the most susceptible 10% of the area contained 55% of total landslides, and the most susceptible 20% of the area explained 70% of all landslides.

The success rate curves indicated that the factors chosen for the landslide susceptibility analyses represented approximately 80% of the factors governing landslide occurrence.

Thus, these results may suggest that the terrain parameters that are considered to be precondition factors represented roughly 80.04 and 83% of the governing factors for both methods and that the triggering factors represented the rest of the influence on landslide occurrence. Therefore, rainfall and seismic data, which were excluded from this study, should be incorporated into future work to obtain better results because these two parameters are known to be the most important triggering factors.

Some minor differences can be found in both the map due to the way applied to determine the weight factors. In the AHP method, weighting the results of each parameter produced a value of 0.029–2.01, while the IV method resulted in values between -2.224 and 1.070. Other differences that are found in both these maps are the values that are undefined in the IV method which produces a map with an empty result and it is not the case of AHP method. Both differences are caused by the natural log formula is applied to the IV method, so the researchers had to give a zero on the final result in order to avoid this problem. Indeed, an assumption has to be made that the undefined value represents no susceptible area to landslide.

Analysis of final result of both maps showed that total weighted values demonstrated significant different range between both methods. The AHP method produced the range between 0.093 and 0.669 while the IV method produced the range between -7.81 and 4.66. The histogram of both models showed different pattern. The AHP method showed four peaks with different frequencies among them (Fig. 7) while the IV method produced one peak (Fig. 8). The different range of minimum and maximum value and the different histograms resulted the different patterns of susceptible areas.

Analysis of curve pattern (Fig. 9) indicated that the AHP represented the underestimation for predicting the future landslide at very high susceptible zone; however, this method showed good prediction of landslide in the high and moderate susceptible areas. It can be seen from the curve of success rate. Success rate of AHP showed insignificant number of landslides on the area at 2–15% most susceptible area. In contrast, IV method showed better prediction on high and very high susceptible areas, but it represented an underestimation at moderate and low susceptible areas compared to AHP. It can be seen from the pattern of the curve that there is still landslide even at the area of moderately susceptible and low susceptible area.

Both maps showed similar patterns of spatial prediction, especially for the northern and eastern parts of the research area. In these models, the very high and the high susceptibility zones covered the upper and middle parts of Kayangan Catchment, and they followed the road and the drainage networks showing the role of the road and drainage networks in increasing the weight value. Both models show that the high and medium susceptibility zones were in the lower part of Kayangan Catchment, which includes plains and gently sloping areas. This phenomenon indicates the overestimation of landslide susceptibility for the plains and gentle slopes due to the presence of the road and drainage networks, which contributed greatly to the weight value, especially in the zones <25 m from the networks. The role of the road network is important because it represents the human intervention to slope modification. In reality, the slope steepness along the road network is higher than that presented on the contour map. The accumulation materials on lower part of the road network are still unconsolidated because this material was placed recently as the consequence of the cutting process for road construction (e.g., Hadmoko 2009 and Hadmoko et al. 2009). In AHP method, it appears that the spatial pattern of susceptible area in the upper catchment is dominated by the road network (<25 m) (Fig. 7c). It is shown by the pattern of susceptible area that clearly follows the road network while in the IV method (Fig. 8c), it appears that some factors influence equally to spatial pattern of susceptibility

zone. The reason was that in AHP method, expert judgment plays a significant role in controlling the weight value and the special attention was paid on the road network at upper catchment due to the significant number of landslides that were associated with the road. The area closest to the road network (<25 m) throughout Kayangan Catchment was considered to have high susceptibility even though that area included the plains and gentle slopes. However, it is important to carefully consider the potential overestimation of landslide susceptibility along the road network that could be caused by the easiness of the mapping processes. This potential overestimation could be minimized through very careful mapping using combination among different approaches, e.g., remote sensing approach, very intensive fieldwork for entire area of the catchment and involving the local people for field guiding.

The information value method appears to have more greatly overestimated susceptibility for the lower part of Kayangan Catchment compared with the AHP method. It is because of the presence of the plains and gentle slope areas that were considered to be medium to very high susceptibility zones, whereas the AHP method presented the better result since it classified those same zones as low to medium susceptibility areas. The expert judgment of AHP seems to be important in this case. Expert judgment on AHP method could provide complementary information since it was based on the field experience of researcher to improve the result of IV method. It is difficult to incorporate expert opinion in IV method because all weighting procedure in IV was purely done based upon the presence of landslide in study area.

Both methods proved good spatial prediction of landslide with only two-year-period landslide inventory data. Therefore, these methods can be applied in different geographic contexts and in different scales. Physical factors such as volcanic or non-volcanic landscapes, slope steepness, and orientation would often be linked to the rainfall occurrence. These physical factors will be the main controlling factors on the variation of the rainfall. Intensive orographic rainfall occurs significantly on very high mountainous region with great variation on slope orientation. Therefore, it would be important to incorporate rainfall data in the future work because the great variation of rainfall event spatially and temporally can play an important role on landslide intensity.

The analysis of the weight value of each parameter for landslide susceptibility indicates that the physical–natural factors were not the only influences on landslide occurrences; human activities also aggravated the probability of landslides and were a triggering factor to landslide occurrences. This phenomenon can be explained by the relation between landslide occurrence and slope steepness. Theoretically, landslide occurrence increases with increasing slope, but at Kayangan Catchment, landslide occurrence increased and reached a maximum value at a slope angle of 20°–30°, and then decreased significantly for slopes greater than 30°. This result is somewhat similar to those of Zhou et al. (2003) on Lantau Island, Hongkong, where the frequency of failures was highest on moderately steep terrain with a gradient ranging from 25° to 35°. Paudel et al. (2007) also correlated landslides and topography on Mt. Aso, Japan, and noted that slopes of 30°–35° were the most exposed areas to landslides. As we observed in Kayangan Catchment, human intervention on the land (agriculture, settlement, infrastructure, or road networks) generally occurs on flat terrain or slopes up to 20°–30°. Slope value >40° are relatively untouched by human activities due to remoteness and the impracticalities of agricultural development.

Although the IV method provided the slightly better prediction (83%) compared to AHP (80%), it has to be noted that AHP can be done with very limited landslide data even in the absence of landslide dataset while the IV method cannot be done without any landslide dataset. The expert judgment procedure in AHP could be an alternative to assess the

landslide susceptible area when the landslide occurrence data are almost unavailable. This method was successfully applied in different regions both in industrialized country such as Spain (e.g., Barredo et al. 2000) and South Korea (e.g., Althuwaynee et al. 2014) and in developing countries such as Nepal (Kayastha et al. 2013) and Iran (Pourghasemi et al. 2012). However, special attention has to be paid during the weighting process because the subjectivity and inconsistency of expert could result the bias of the result. However, this disadvantage can be reduced by incorporating consistency ratio test before introducing the weight value during the analysis. IV method depends largely on the quality of landslide data. The imprecise and incomplete data of landslide location included the shape, and the area could a major limitation to assess the susceptible area (Schicker and Moon 2012).

The results of this study would be valuable to the local government to support decision making concerning disaster risk reduction. There are a limited number of studies related to landslide hazard and risk assessment conducted in the study area; therefore, this work can serve as a reference and be extended to other areas in Indonesia. Since the AHP method requires less data and simple in operation, it can be a good solution for the developing countries like Indonesia. It can be applied on inaccessible remote region where the landslide data are still unavailable. The expert opinion is one of the best solutions to determine the weight value of parameter maps that contribute to landslide occurrence. However, field experiences and good understanding on the physical characteristic of the study area are needed to produce the reliable susceptible map. In addition, due to the great variation of geology and land use in Indonesia, any weighting value resulted in this study should not be automatically introduced for another location in this country. The weight value has to be adapted with the study area.

The statistical model used in this study is relatively simple and resulted in good estimation; therefore, this approach can then be implemented in developing countries such as Indonesia due to the practicality and the relatively inexpensive cost of these methods. However, some conditions and some adjustments have to be followed. The application of IV depends largely on the availability of landslide data and on the accessibility of the study area. Therefore, the researcher would suggest to apply this method at urban and peri-urban areas where the landslides data are available and the area is easily accessible that allow the government collect the landslide data.

Because this work was intended to evaluate the spatial probability of landslides (susceptibility), the temporal probability of landslides was not incorporated due to the limitations of multi-temporal landslide data and the lack of rainfall data, the main triggering factor for landslides. Therefore, the “real” hazard map, as defined by Varnes (1984), cannot be provided by this study. As a result, the triggering factors and the multi-temporal landslide data should be incorporated in future research to assess the integrated spatiotemporal landslide probability so that the “real” hazard map can be provided.

6 Conclusion

This study provided an integrated analysis of spatial landslide behavior and its correlation with terrain parameters as the primary conditioning factors of landslides to determine the spatial pattern of susceptibility zones of landslides. Our analysis demonstrated that the terrain parameters contributed differently to landslide occurrence, as indicated by the frequency and density of landslides corresponding with each terrain parameter. The results showed that human activities play a major role in landslide occurrence, particularly

through slope cutting for houses and road construction, as indicated by the high susceptibility area within close proximity to the roads.

A semiquantitative approach and bivariate statistical model were applied to build landslide susceptibility maps: the AHP and information value methods. Both models provided good prediction accuracy for susceptibility, explaining approximately 80% of landslide occurrences. The information value method gave better spatial prediction results. The advantage of information value method is that the negative weight can be resulted as a consequence of the negative contribution of each parameter to landslide susceptibility. The disadvantage of the information value is that the absence of landslide yielded the zero value that can result in undefined value (∞) for the final result. Therefore, the latter has to be assigned to zero. However, the IV method cannot be applied for the area where the landslide data are unavailable while the AHP method can be used with no landslide data available. The prediction was conducted by expert opinion that allows us to determine the weight value. The subjectivity and inconsistency during the weighting process can be eliminated by applying the consistency ratio.

In spite of some limitations appearing in these approaches, both methods can be applied in developing countries like Indonesia to spatially determine the landslide susceptibility. They can be applied for the larger area with some consequences that have to be considered, e.g., more volume of data and more field works have to be done.

This study does provide the spatial probability of landslides, which is essential for landslide hazard assessment and risk assessment. This domain has become an important issue in spatial planning due to the increasing impact of recent disasters in Indonesia. Because few Indonesian scientists are working on these methods, this study could be very useful for risk management and for the development of natural hazard studies in the future. In addition, the scientific products resulted from this research has to be communicated and discussed with local authorities in order apply the result on landslide disaster mitigation program. Both maps provided two different looking-like maps in terms of spatial pattern; therefore, comprehensive guideline have to be done to make the maps are applicable at operational level. Firstly, the susceptibility map should be incorporated with the technical guidance and short training on how to read and to interpret the map. Secondly, the digital map should be used for decision making; therefore, the local authorities can identify the susceptible area in pixel basis.

Acknowledgements Author acknowledges Beasiswa Unggulan, Indonesian Ministry of Education and Culture through P2D program, for financial support, Research Centre for Disasters, and Faculty of Geography Universitas Gadjah Mada, Indonesia, for the facilities during data processing and providing financial support through Small Research Grant Project and UMR 8591 CNRS Laboratoire de Géographie Physique, 1 place A. Briand, 92195 Meudon Cedex, France, for data processing. The author is also grateful to the anonymous reviewers for their valuable comments on the manuscript.

References

- Ahmed A, Brahmantyo B, Ugai K (2013) On the Tasikmalaya earthquake induced landslide in Indonesia: field investigation. In: Ugai K et al (eds) Earthquake-induced landslides. Springer, Berlin Heidelberg, pp 253–260
- Aleotti P, Chowdhury P (1999) Landslide hazard assessment: summary review and new perspectives. Bull Eng Geol Environ 58:21–44
- Althuwaynee OF, Pradhan B, Park HJ, Lee JH (2014) A novel ensemble bivariate statistical evidential belief function with knowledge-based analytical hierarchy process and multivariate statistical logistic regression for landslide susceptibility mapping. Catena 114:21–36

- Barredo JI, Benavides A, Hervas J, van Westen CJ (2000) Comparing heuristic landslide hazard assessment techniques using GIS in the Tirajana basin, Gran Canaria Island, Spain. *Int J Appl Earth Obs Geoinform* 2(1):9–23
- Brabb EE (1984) Innovative approaches to landslide hazard mapping. In: *Landslides-Glissements de Terrain, IV international symposium on landslides*, vol 1. Toronto, pp 307–323
- Carrara A (1983) Multivariate models for landslide hazard evaluation. *Math Geol* 15:403–426
- Carrara A, Cardinali M, Detti R, Guzzetti F, Psqui V, Reichenbach P (1991) GIS techniques and statistical models in evaluating landslide hazard. *Earth Surf Process Landf* 16:427–445
- Carrara A, Cardinali M, Guzzetti F, Reichenbach P (1995) GIS technology in mapping landslide hazard. In: Carrara A, Guzzetti F (eds) *Geographical information systems in assessing natural hazards*. Kluwer Academic Publishers, Dordrecht, pp 135–175
- Carson MA, Kirkby MJ (1972) *Hillslope form and process*. Cambridge University Press, London
- Castellanos Abella EA, Van Westen CJ (2007) Generation of a landslide risk index map for Cuba using spatial multi-criteria evaluation. *Landslides* 4(4):311–325
- Castellanos Abella EA, Van Westen CJ (2008) Qualitative landslide susceptibility assessment by multi-criteria analysis: a case study from San Antonio del Sur, Guantánamo, Cuba. *Geomorphology* 94(3–4):453–466
- Chau KT, Sze YL, Fung MK (2004) Landslide hazard analysis for Hong Kong using landslide inventory and GIS. *Comput Geosci* 30(4):429–443
- Chung CF, Fabbri A (1998) Three Bayesian prediction models for landslide hazard. In: Buccianti A (ed) *Proceedings of international association for mathematical geology. IAMG'98. Ischia*, pp. 204–211
- Chung CF, Fabbri A (1999) Probabilistic prediction models for landslide hazard mapping. *Photogramm Eng Remote Sens* 65(12):1389–1399
- Chung CF, Fabbri A, Van Westen CJ (1995) Multivariate regression analysis for landslide hazard zonation. In: Carrara A, Guzzetti F (eds) *Geographical information systems in assessing natural hazards*. Kluwer Academic Publishers, Dordrecht, pp 107–133
- Dai FC, Lee CF, Ngai YY (2002) Landslide risk assessment and management: an overview. *Eng Geol* 64:65–87
- Das I, Stein A, Kerle N, Dadhwal VK (2012) Landslide susceptibility mapping along road corridors in the Indian Himalayas using Bayesian logistic regression models. *Geomorphology* 179:116–125
- Dhakal AS, Amada T, Aniya M (1999) Landslide hazard mapping and the application of GIS in the Kulenkhani watershed, Nepal. *Mt Res Dev* 19(1):3–16
- Duque A, Echeverría G, Fernández E, Kerejeta A, Cendrero A, Díaz de Terán JR, Tamés P (1991) A methodological approach for the development of predictive models for hazard assessment. In: Panizza M, Soldati M, Coltellacci MM (eds) *Proceedings european experimental course on applied geomorphology*, vol 2., Instituto di geologiaUniversità degli Studi di Modena, Modena, pp 13–25
- Faris F, Fawu W (2014) Investigation of the initiation mechanism of an earthquake-induced landslide during rainfall: a case study of the Tandikat landslide, West Sumatra, Indonesia. *Geoenviron Disasters* 1:4
- <ftp://ftp.itc.nl/pub/ilwis/ilwis30/pdf/chap10.pdf>, consulted on 1 July 2013
- García-Rodríguez MJ, Malpica JA, Benito B, Díaz M (2008) Susceptibility assessment of earthquake-triggered landslides in El Salvador using logistic regression. *Geomorphology* 95:172–191
- Glade T, Crozier MJ (2005) A review of scale dependency in landslide hazard and risk analysis. In: Glade T, Anderson M, Crozier MJ (eds) *landslide hazard and risk*. Wiley, Chichester, pp 75–138
- Hadmoko DS (2009) Les mouvements de terrain dans les Monts Menoreh: variabilité spatio-temporelle, impacts, déclenchement, et analyse de la susceptibilité. Ph.D. thesis. Université Paris 1 Panthéon Sorbonne
- Hadmoko DS, Lavigne F, Sartohadi J, Samodra G, Christanto N (2009) GIS application for comprehensive spatial landslides analysis in Kayangan Catchment, Menoreh Mountains, Java, Indonesia. In: Malet JP, Rémaitre A, Bogaard T (eds) *Landslides processes: from geomorphic mapping to dynamic modeling*. European Center of Geomorphological Hazards, Strasbourg, pp 297–302
- Hadmoko DS, Lavigne F, Sartohadi J, Hadi MP (2010) Landslide hazard and risk assessment and their application in risk management and landuse planning in eastern flank of Menoreh Mountains, Yogyakarta Province, Indonesia. *Nat Hazards* 54(3):623–642. doi:10.1007/s11069-009-9490-0
- He Y, Beighley RE (2008) GIS-based regional landslide susceptibility mapping: a case study in southern California. *Earth Surf Process Landf* 33:380–393
- Irigaray C, Fernández T, Chacón J (1996) Comparative analysis of methods for landslide susceptibility mapping. In: Chacón J, Irigaray C, Fernández T (eds) *Landslides*. Balkema, Rotterdam, pp 373–384
- Irigaray CF, Del Castillo TF, El Hamdouni R, Montero JC (1999) Verification of landslide susceptibility mapping: a case study. *Earth Surf Process Landf* 24:537–544

- Jade S, Sarkar S (1993) Statistical model for slope instability classifications. *Eng Geol* 36:71–98
- Kayastha P, Dhital MR, De Smedt F (2013) Application of the analytical hierarchy process (AHP) for landslide susceptibility mapping: a case study from the Tinau watershed, west Nepal. *Comput Geosci* 52:398–408
- Kendall M, Stuart A (1979) *The advanced theory of statistics: inference and relationship*. Griffin, London, p 748
- Khan YA, Lateh H (2011) Failure mechanism of a shallow landslide at Tun-Sardon road cut section of Penang Island, Malaysia. *Geotech Geol Eng* 29:1063–1072
- Lee S, Talib JA (2005) Probabilistic landslide susceptibility and factor effect analysis. *Environ Geol* 47(7):982–990
- Marfai MA, King L, Singh LP, Mardiatno D, Sartohadi J, Hadmoko DS (2008) Natural hazard in central Java. *Environ Geol* 56:335–351
- Mulder HF (1991) In: Mulder HF (ed) *Assessment of landslide hazard*, Faculty of Geographical Science. University of Utrecht, The Netherlands
- Oh HJ, Lee S, Soedradjat GM (2010) Quantitative landslide susceptibility mapping at Pemalang area, Indonesia. *Environ Earth Sci* 1(6):1317–1328
- Ohlmacher GC (2007) Plan curvature and landslide probability in regions dominated by earth flows and earth slides. *Eng Geol* 91:117–134
- Paudel PP, Omura H, Kubota T, Inoue T (2007) Spatio-temporal patterns of historical shallow landslides in a volcanic area Mt. Aso, Japan. *Geomorphology* 88:21–33
- Pourghasemi HR, Pradhan B, Gokceoglu C (2012) Application of fuzzy logic and analytical hierarchy process (AHP) to landslide susceptibility mapping at Haraz watershed, Iran. *Nat Hazards* 63:965–996
- Rahardjo W, Rumidi S, Rosidi HMD (1995) *Peta Geologi Lembar Yogyakarta, Jawa*. Pusat Penelitian dan Pengembangan Geologi, Bandung. (Geological map of Yogyakarta, Java)
- Remondo J, González-Diez A, Diaz de Terán JR, Cendrero A (2003) Landslides susceptibility models utilising spatial data analysis techniques. A case study from the lower Deba Valley, Guipúzcoa (Spain). *Nat Hazards* 30:267–279
- Saaty TL (1980) *The analytic hierarchy process: planning, priority setting, resource allocation*. McGraw-Hill Book Co, New York, p 287
- Saaty TL, Vargas LG (2001) *Models, methods, concepts and applications of the analytic hierarchy process*. Kluwer, Dordrecht, p 333
- Saha AK, Gupta RP, Arora MK (2002) GIS-based landslide hazard zonation in the Bhagirathi (Ganga) Valley, Himalayas. *Int J Remote Sens* 23(2):357–369
- Saha AK, Gupta RP, Sarkar I, Arora MK, Csaplovics E (2005) An approach for GIS based statistical landslide susceptibility zonation: with a case study in the Himalayas. *Landslides* 2:61–69
- Schicker R, Moon V (2012) Comparison of bivariate and multivariate statistical approaches in landslide susceptibility mapping at a regional scale. *Geomorphology* 161–162:40–57
- Slide RC, Ochiai H (2006) *Landslides: processes, prediction and landuse*. Water Resources Monograph 18, American Geophysical Union, Washington, DC
- Terlien MTJ (1996) *Modelling spatial and temporal variations in rainfall-triggered landslides*. Ph.D. Thesis. ITC Enschede, the Netherlands
- Thiery Y, Malet JP, Sterlacchini S, Puissant A, Maquaire O (2007) Landslide susceptibility assessment by bivariate methods at large scales: application to a complex mountainous environment. *Geomorphology* 92:38–59
- Van Den Eeckhout M, Vanwalleghem T, Poesen J, Govers G, Verstraeten G, Vandekerckhove L (2006) Prediction of landslide susceptibility using rare events logistic regression: a case-study in the Flemish Ardennes (Belgium). *Geomorphology* 76:392–410
- Van Westen CJ (1993) *Application of geographic information systems to landslide hazard zonation*. Ph.D. Thesis, Technical University Delft. ITC-Publication Number 15, ITC, Enschede, The Netherlands
- Van Westen CJ, Rengers N, Soeters R (2003) Use of Geomorphological Information in Indirect Landslide Susceptibility Assessment. *Natural Hazards* 30:399–419
- Van Westen CJ, Van Ach TWJ, Soeters R (2005) Landslide hazard and risk zonation: Why is still so difficult ? *Bull Eng Geol Environ* 65:167–184
- Van Westen CJ, Castellanos E, Kuriakose SL (2008) Spatial data for landslide susceptibility, hazard, and vulnerability assessment: an overview. *Eng Geol* 102(3–4):112–131
- Varnes DJ (1984) *Landslide hazard zonation: a review of principles and practice*. Commission on landslides of the IAEG, UNESCO, Natural Hazards No. 3
- Yalcin A (2007) GIS-based landslide susceptibility mapping using analytical hierarchy process and bivariate statistics in Ardesen (Turkey). *Catena* 72(1):1–12

- Yalcin A (2008) GIS-based landslide susceptibility mapping using analytical hierarchy process and bivariate statistics in Ardesen (Turkey): comparisons of results and confirmations. *Catena* 72:1–12
- Yalcin A, Bulut F (2007) Landslide susceptibility mapping using GIS and digital photogrammetric techniques: a case study from Ardesen (NE-Turkey). *Nat Hazards* 41:201–226
- Yin KJ, Yan TZ (1988) Statistical prediction model for slope instability of metamorphosed rocks. In: *Proceedings 5th international symposium on landslides, vol 2. Lausanne*, pp 1269–1272
- Zhou G, Esaki T, Mitani Y, Xie M, Mori J (2003) Spatial probabilistic modeling of slope failure using an integrated GIS Monte Carlo simulation approach. *Eng Geol* 68:373–386